AIMS Bioengineering

AIMS Bioengineering, 12(4): 613–637.
DOI: 10.3934/bioeng.2025028
Received: 24 September 2025
Revised: 30 November 2025
Accepted: 03 December 2025
Published: 09 December 2025

https://www.aimspress.com/journal/Bioengineering

Research article

Translational design and clinical validation of a non-invasive glucose monitor based on oxygen saturation and heart rate signals

Mustafa F. Mahmood*, Suhair M. Yaseen and Saleem Latteef Mohammed

Department of Medical Instrumentation Techniques Engineering, Electrical Engineering Technical College, Middle Technical University, Baghdad, Iraq

* **Correspondence:** Email: mustafa.falah@mtu.edu.iq; Tel: +9647707979514.

Abstract: Diabetes is a chronic disorder that is among the most prevalent diseases in many parts of the world, as it is brought about by high levels of sugar in the blood, which may cause severe complications in the heart, blood vessels, kidneys, and nerves. Thus, it is important to monitor blood glucose continuously. The use of traditional finger-prick methods was done away with in this study, and it was substituted with a noninvasive blood glucose meter. The proposed system has an optical sensor known as the MAX30100, an LCD, and an Arduino Mega 2560 microprocessor to provide real-time measurements. The device can determine the glucose content through a combination of digital filtering and mathematical computations implemented within the microcontroller through the correlation of heart rate (HR) and oxygen saturation (SpO_2). The 120 samples (females and males, fasting, normal, and diabetic) were tested with the system and compared with a commercial reference device (Accu-Chek). There were high accuracy levels of 97.5% agreement, a sensitivity of 97.94%, and a specificity of 95.65%. Strong correlations were found. HR was negatively correlated with SpO_2 ($r = -0.936$, $p < 0.001$) and positively correlated with glucose ($R^2 = 0.860$, $p < 0.001$). The validity and clinical reliability of the system were validated by statistical methods such as the Clarke error grid, Bland–Altman test, and error test. The suggested approach showed promise as a practical and affordable substitute for regular blood glucose monitoring, and it achieved greater accuracy than that in earlier research.

Keywords: Arduino Mega 2560; Clarke error grid analysis; noninvasive glucose; MAX30100 sensor; statistical analyses

1. Introduction

One of the most common endocrine disorders worldwide, diabetes mellitus (DM), is characterized by chronic hyperglycemia, or increased blood sugar. Poor cellular sensitivity to insulin causes Type 2 DM, whereas inadequate insulin production causes Type 1 DM [1–3]. Metabolic dysregulation involving carbohydrates, proteins, and lipids is a result of both forms of diabetes. Traditional signs of diabetes include blurred vision, weight loss, polydipsia (excessive thirst), and polyuria (excessive urine). If left uncontrolled, diabetes may cause severe complications, including kidney failure, neuropathy, retinopathy, peripheral and coronary artery disease, heart failure, and stroke [4,5]. Globally, the prevalence of diabetes has increased dramatically. In 1990, only about 7% of adults (≥18 years) were affected; however, this number doubled to 14% by 2022. In 2021, approximately 1.6 million deaths were due to diabetes and approximately 47% of them were in those under the age of 70 years [6,7]. Considering this threatening trend, in order to enhance the survival of the patient and avoid complications, it is important to employ effective and accurate methods of monitoring blood glucose. A key component of treating diabetes is ensuring that the blood glucose level stays as close to the safe physiological limits as feasible [8].

Finger-prick tests and other conventional invasive glucose monitoring methods are helpful, but they have several drawbacks, such as pain and needle anxiety [9], as well as infection risk, delayed wound healing in diabetics [10], and low patient compliance. Noninvasive glucose testing methods have developed more quickly as a result of these restrictions. Newer methods include microwave sensors that measure glucose levels by examining the phase changes and attenuation of reflected waves [11–18], photometric sensors, and electromagnetic sensors [19–21]. Noninvasive glucose meter design has been the subject of numerous investigations. An Arduino UNO R3 microcontroller, a noninverting AC amplifier and filter circuit, an LCD, and a TCRT1000 reflecting optical sensor operating close to the infrared region at 950 nm are the four primary parts of a device created by Preya Anupongongarch et al. They obtained a 95% accuracy rate with their system [22]. In a similar vein, Alam et al. suggested a glucometer that allows remote monitoring by integrating Internet of Things (IoT) technology with an 850-nm infrared light-emitting diode (LED) and a visible red laser. When tested on 198 participants between the ages of 20 and 60, the accuracy rate of the method was 96% [23]. To measure blood glucose selectivity, Sivakumar et al. developed a system that combines a 630-nm red LED, a 940-nm near-infrared (NIR) LED sensor, and a BPW34 photodiode array with signal conditioning circuits and optimized optical cuvettes, with encouraging results [24].

Kiani et al. [25] described a microwave substrate integrated waveguide resonator sensor to monitor blood glucose concentration noninvasively as cost-effective and pain-free equipment utilized by diabetics. This sensor involves the use of microwave technology to be able to ensure precise determination of the glucose levels without invasive procedures. The device has a high level of sensitivity and reliability, and hence it is a promising alternative for continuous, noninvasive glucose monitoring. To meet the main concerns of diabetic care, including the cost, comfort, and user-friendliness, its design suits portable applications. These findings show that sensors based on microwaves can provide accurate measurements and can form a possible solution as next-generation glucose monitoring devices. Kiani et al. [26] introduced a dual-frequency microwave resonance sensor to detect a change in the glucose levels in noninvasive sensing of the fingertip. The sensor has two frequencies, which increase the sensitivity to dielectric changes due to glucose. It allows continuous monitoring in real time without blood sampling and it is highly accurate and reliable. The dual-

frequency method has better detection properties and thus it is a potential solution for noninvasive measurement of glucose.

Herlambang and Arifin [27] presented a method for measuring blood sugar levels by using noninvasive technology. The system involves an Arduino Nano, a MAX30100 sensor, and an organic light-emitting diode (OLED). The experimental result showed that the system was able to measure blood sugar levels by noninvasive technology with an accuracy of 94.3%. Islamudin et al. [28] offered a method for measurement blood sugar levels by using noninvasive expertise with the IoT. The system involves an Arduino (ESP8266), a MAX30102 sensor, and OLEDs. The experimental result showed that the system was able to measure blood sugar levels by noninvasive technology with an accuracy of 93.97%. The systems have a low cost and real-time results. However, the sample size was not mentioned, nor was the sample classified in terms of disease type (normal or diabetic). Other studies have confirmed the ability to measure blood glucose levels, but without any results, using MAX30100 and MAX30102 [29–32]. This present study's primary contributions are as follows:

- We developed and put into use a low-cost, portable tool for noninvasive blood glucose monitoring.
- On the basis of heart rate (HR) and oxygen saturation (SpO_2), the MAX30100 sensor was used to estimate the glucose content.
- We designed a new algorithm for data analysis and signal processing that is integrated into the control unit.
- We validated the accuracy of the proposed device against a benchmark device (BM) glucometer using rigorous statistical methods.

The suggested noninvasive prototype uses the MAX30100 optical sensor and specific calibration and signal-processing software to approximate blood glucose levels. This combination enables quick and painless measurement and gives a reliable and inexpensive option for both diabetic and nondiabetic users. The remainder of this paper is organized as follows: Section 2 presents the design of the proposed system. Section 3 describes the data collection process. Section 4 explains the experimental setup and configurations. Section 5 discusses the evaluation metrics and statistical analyses. Section 6 presents and analyzes the results. Finally, Section 7 concludes the paper and outlines directions for future work.

2. System configuration

The suggested system's block diagram, which is powered by an external 9-V battery and comprises a liquid crystal display (LCD), an Arduino Mega 2560 microprocessor, and a MAX30100 optical sensor, is shown in Figure 1. Data collection and processing are both handled by the microcontroller, which also provides power to the sensor and display. The patient applies a fingertip to the MAX30100 sensor while it is operating. The sensor emits light at 660 nm (red) and 880 nm (infrared), and a photodiode detects the reflected signal. Variations in reflected and absorbed light are caused by blood analytes and tissue properties.

To isolate the glucose-related component, three methods were implemented. The first was optical absorption ratio analysis, where the absorption intensities at 660 nm and 880 nm were measured, and their ratio was calculated (Equation 1).Second, in alternating current–direct current (AC/DC) signal separation, raw signals were pre-processed to remove noise and then decomposed into an AC component (a pulsatile signal representing heartbeats and capillary blood volume changes) and a DC

component (baseline absorption from the tissue and skin). As shown in Equation 2, the glucose-dependent absorption ratio was computed. For mathematical modeling of the physiological link between glucose concentration using SpO_2 and HR, a proprietary algorithm was created. Using the MAX30100 library, bio-signals were recovered, and the moving average filter (Equation 3) was used to reduce noise. Using reference device data, an initial glucose estimate was manually generated using the filtered HR and SpO_2 values(Equation 4) [33–35]. In this multi-stage strategy, mathematical modeling, physiological modeling, and optical modeling are combined to improve the accuracy of glucose estimation.

$$R=\frac{I_{RED}}{I_{IR}} \tag{1}$$

$$A=\frac{Variable\ Signal}{Constant\ Signal} \tag{2}$$

$$HR_{filt}=HR_{read}\sum_{read=1}^{N}\frac{1}{N} \tag{3}$$

$$Glucose_{value}=a\times HR_{filt}+b \tag{4}$$

where R is the difference between the two concentrations as a ratio, I_{RED} represents the signal intensity at a wavelength of 660 nm, I_{IR} represents the signal intensity at 880 nm, A acts as the absorption ratio, HR_{filt} represents the HR value using a filter, HR is the heart rate value measured using a sensor, N is the filter size; $Glucose_{value}$ is the glucose value. The values a and b were extracted for the calibrated linear equations using 120 samples of different ages and genders, including nondiabetic, diabetic, and fasting patients.

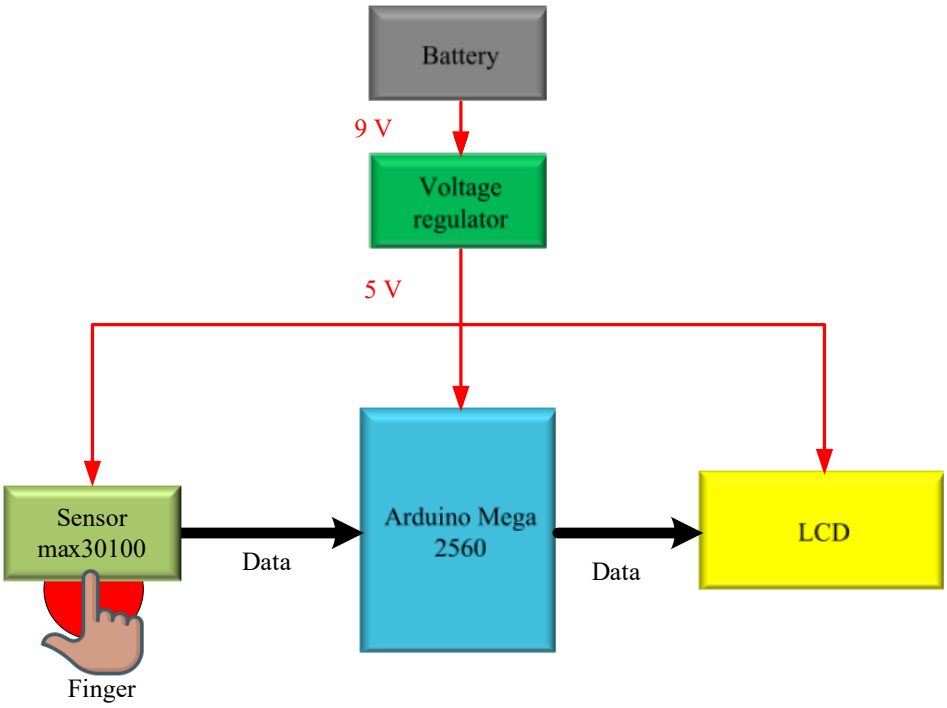

Figure 1. Block diagram of the proposed system.

The MAX30100 sensor operates with two wavelengths: 660 nm (red) and 880 nm (infrared) [36]. The degree of absorption of light at these wavelengths depends on the oxygenation of hemoglobin (Hb). In the infrared spectrum, deoxygenated Hb absorbs more red light than oxygenated hemoglobin (HbO_2) [37–43]. During heartbeats, photoplethysmography (PPG) signals are produced when the pulsatile flow of arterial blood causes variations in the measured light intensity. The goal of this signal is to extract SpO_2 and HR. While HR variability (HRV) indices can be obtained from the raw information provided by the MAX30100 sensor, only HR and SpO_2 were utilized in this investigation to forecast glucose levels. HRV indicators were not examined in this analysis to prevent broadening the study's scope or adding more confounding variables. Calculating the ratio of red to infrared light absorption—which changes with blood oxygenation—is the foundation of pulse oximetry. It is possible to measure SpO_2 by comparing the transmitted or reflected light at the two wavelengths (Figure 2). Blood with low oxygen has greater absorption at 660 nm and higher absorption at 880 nm. In the reflective arrangement, the sensor uses a photodiode to detect the signal in addition to the LEDs to gather the signals in the MAX30100 sensor [44].

The recent research has proposed that the variation in light absorption at various wavelengths also depends on the glucose concentration, as it affects the refractive index and the viscosity of blood [44–48]. Namely, glucose exhibits peculiar absorptive properties in the NIR region (approximately 950 nm). At short wavelengths (660 nm), glucose absorbs more than water but at long wavelengths (880 nm), the absorption of water increases drastically. This relationship is crucial because water makes up 60–70% of bodily tissue and has a significant impact on how light travels through biological media [49,50]. The absorption curves of glucose and water are shown in comparison in Figure 3, emphasizing the spectrum overlap and the significance of choosing the measurement wavelengths properly. Although the -nm infrared signal provides sensitivity to changes in oxygenation, the proposed method uses the 660-nm red signal as a baseline to take background interference into account. When these signals are combined, SpO_2 may be estimated and characteristics linked to glucose can be extracted from the PPG waveform.

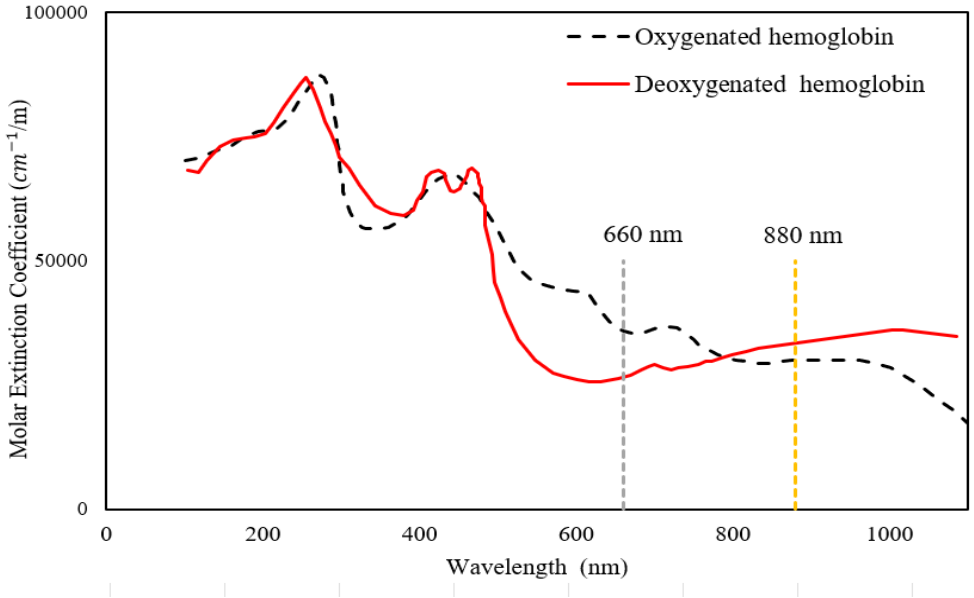

Figure 2. Relationship between the molar extinction coefficient and wavelength.

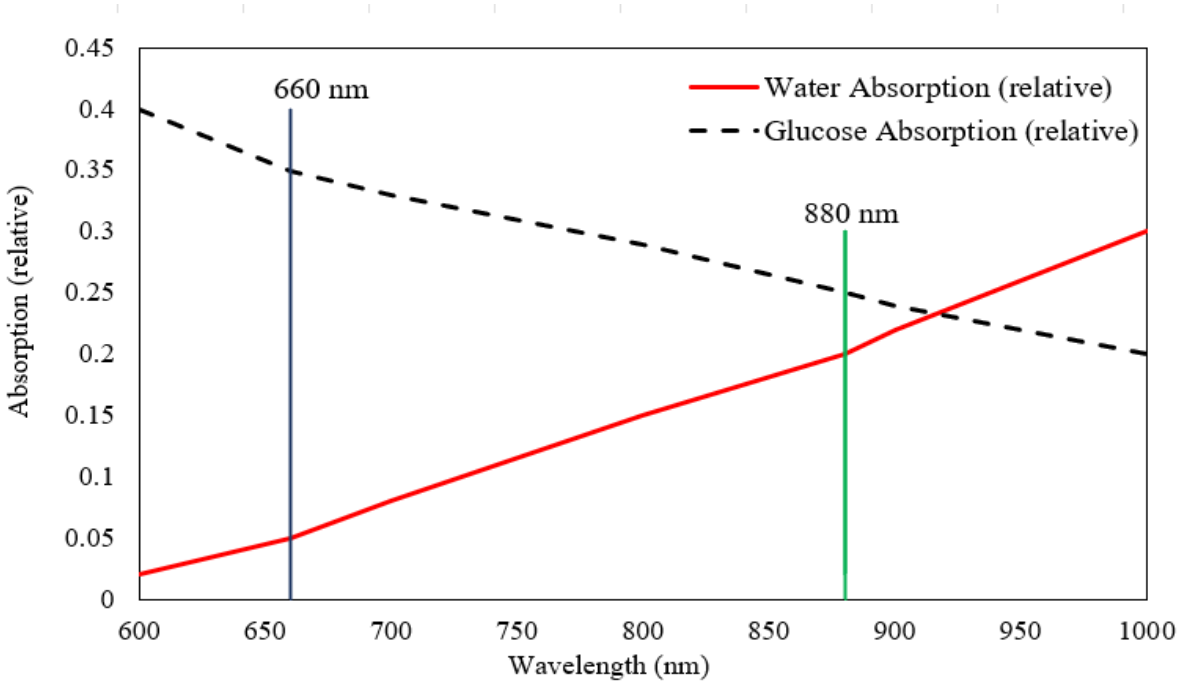

Figure 3. Relationship between absorption and wavelength for water and glucose**.**

Various frequency bands and sensing domains are also explored in the area of noninvasive glucose monitoring, with different benefits and drawbacks. The current methods can broadly be divided into three groups. NIR spectroscopy (650–1000 nm) is popular because it penetrates through the tissue layers. This technique detects a greater number of chemical constituents than any alternative method [51]. Its advantages include low cost, small sensors, and that it can be used in wearable devices. The limitations include intense interference by the absorption of water, low glucose specificity and susceptibility to ambient light [52]. Mid-infrared spectroscopy (2500–10000nm) offers highly accurate and direct evaluations of the molecular absorption characteristics of glucose [53]. The benefits include its great biochemical specificity; the limitations are costly equipment, shallow penetration, and that it cannot be used in a portable system [54]. Research into microwave and radio-frequency sensors is currently underway as these are deeper penetrators and are more sensitive to dielectric variations in tissue [55]. It benefits are the ability to work without any physical contact and high sensitivity to changes in the dielectric properties of glucose. The limitations are its complicated sensor design, environmental interference, and restrictions at higher power levels [56,57].

Although these approaches are very varied, NIR spectroscopy-based optical sensing is one of the most viable ways to have low-cost and portable systems. Thus, the suggested system embraces dual-wavelength NIR spectroscopy sensing (660 nm and 880 nm) with the support of custom signal-processing and statistical modeling to offer a trade-off among usability, price, and physiological sensitivity.

3. Data collection

The distribution of study participants is shown in Figure 4. In total, 120 volunteers (65 men and 55 women) of various ages were enlisted. A systematic questionnaire was used to assess the health

state of the participants, who included 21 diabetic patients, 64 fasting people, and 35 healthy controls. Each volunteer was measured once using both the proposed noninvasive device and the BM under identical environmental conditions and at the same time of day. In certain cases, the measurement was repeated when abnormal readings were observed. Some readings that initially appeared to be excessively high were re-tested and later confirmed to be accurate upon comparison with the BM. This procedure ensured direct statistical comparison and validation of the proposed system against the BM. Although traditional finger-prick blood glucose meters provide results within seconds of inserting the test strip, there are manual procedures involved. The proposed system provides an estimated glucose level in approximately 2 minutes. The MAX30100 sensor acquired fingertip PPG signals at a sampling frequency of 100 Hz for 30 seconds per trial.

It should be noted that the sample size (120 subjects) is relatively limited; however, it was sufficient for initial validation and proof-of-concept demonstration. Future studies with larger and more diverse cohorts will be required to establish the generalizability of the proposed system further. Everything was measured under controlled conditions in an indoor environment at room temperature (22–25 °C). All measurements were taken while the participants were at rest to ensure the HR signals' stability and to minimize variability. We made sure to inform all participants about the purpose of the research and the method we would use to collect data. We emphasized that the data would be used for scientific purposes only and that the information would remain confidential and secure. As a result, all participants agreed to participate in the study and share their data with us voluntarily and knowingly. We used the traditional method and the proposed system for each participant to measure blood glucose levels.

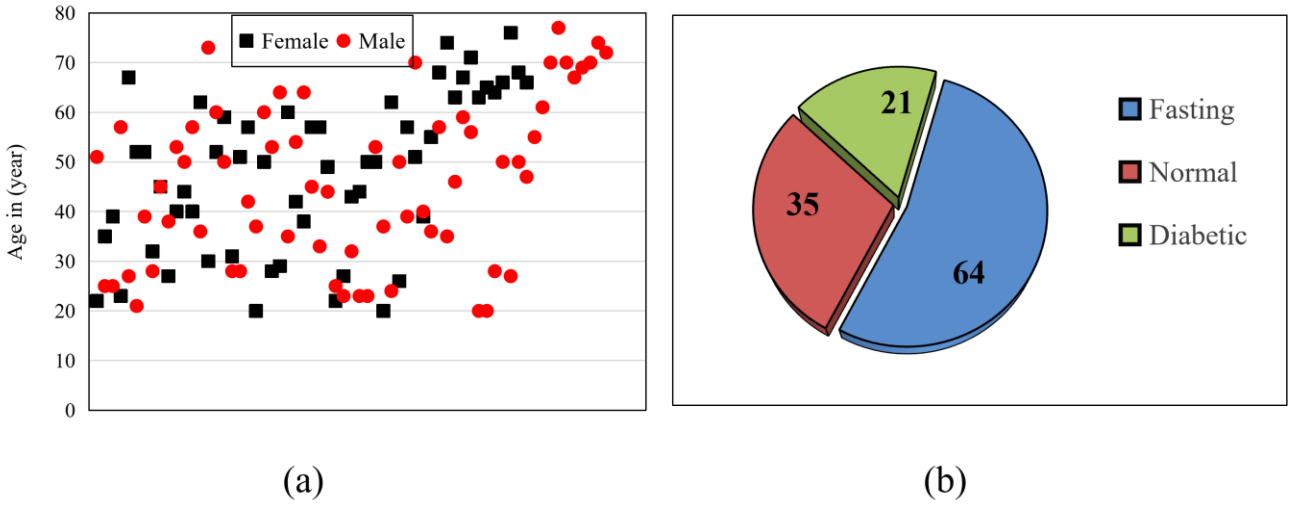

Figure 4. Distribution of the samples (a) according to age and gender, and (b) according to the nature of the person (fasting, diabetic, and nonfasting (normal) persons).

4. Experimental setup

An LCD, an Arduino Mega 2560 microprocessor, and a MAX30100 optical sensor were all integrated into the suggested system (Figure 5). The MAX30100 sensor was used because it measures SpO_2 and HR values based on red light at 660 nm and infrared at 880 nm, as it is a light sensor with

enhanced optics and a low-noise analog signal processor [50,58]. For the sensor to function, two supply voltages of 1.8 V and 3.3 V are normally needed [59]. This system uses low-pass digital filtering and a moving average filter to reduce noise in the raw signals that are sent to the microcontroller with a mathematical model, then uses the HR and SpO_2 measurements to estimate the blood glucose concentration (Equations 2–4). The Arduino Mega 2560 microcontroller's accessibility, affordability, and ease of use led to its selection. A 16-MHz crystal oscillator, four Universal Asynchronous Receiver/Transmitter ports, an In-Circuit Serial Programming connector, sixteen analogue inputs, a USB interface, and 54 digital input/output (I/O) pins—15 of which can be set up as pulse width modulation outputs—are among its features [60–63]. These specifications facilitate real-time data acquisition, signal pre-processing, and algorithm execution.

The LCD is a mix of both liquid and crystal to display the glucose reading in real-time to the user. The sensor was covered with an opaque fingertip cover to reduce ambient light to minimize interference, and more digital filtering was done to reduce motion artifacts. The system's flowchart is displayed in Figure 6. HR and SpO_2 signals are obtained and filtered when the finger is put on the sensor; if the signal quality is insufficient, the user is asked to move the finger. Once the processed data has been run through the glucose estimation algorithm, the estimated glucose concentration is displayed on the LCD. The MAX30100 was chosen for its tiny size; compatibility with portable, low-cost systems; and affordability in Iraq. Although a pre-made sensor was utilized, custom algorithms were developed to increase accuracy and reliability beyond the usual library functions. To reduce temporal fluctuations, the average HR during a 30-second stable recording period was used to estimate glucose levels rather than instantaneous HR values.

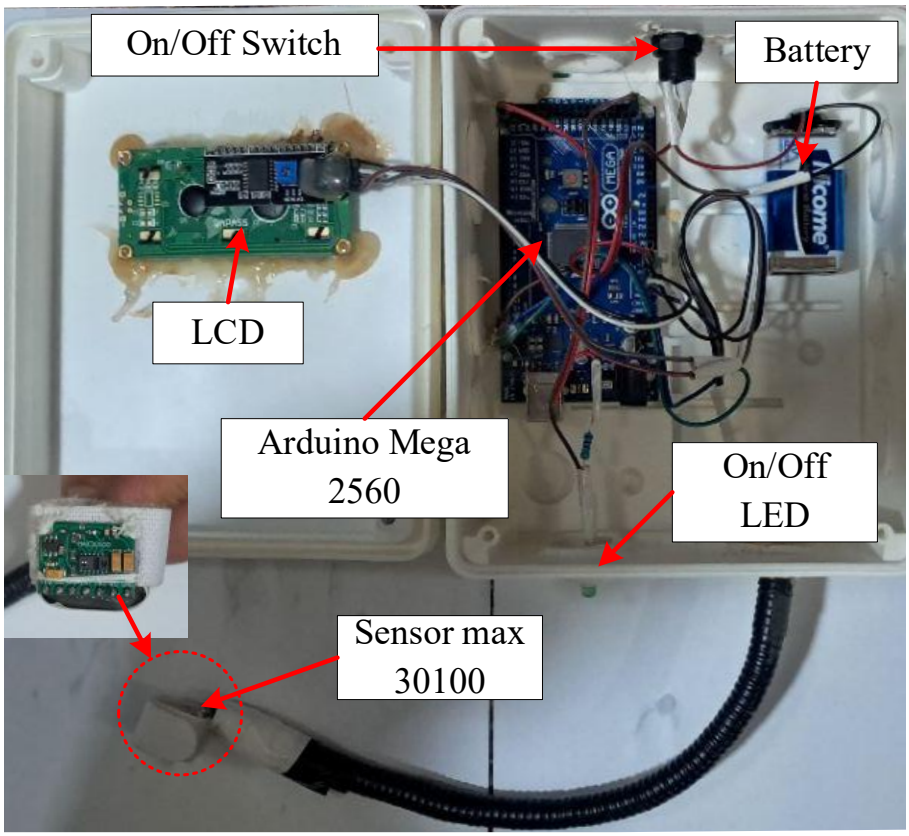

Figure 5. Snapshot of the components of the proposed system.

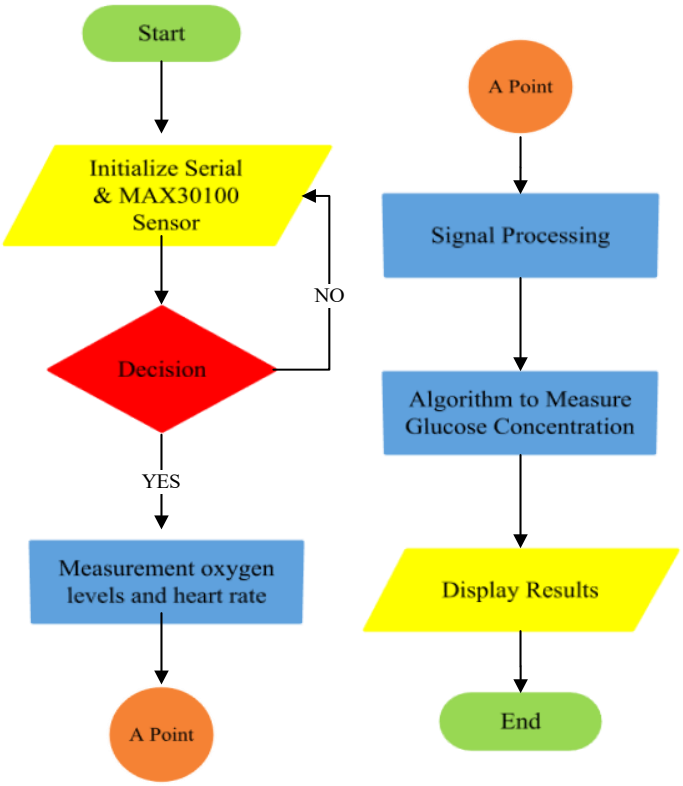

Figure 6. Flowchart of the proposed system.

To improve signal quality and reduce possible error sources, digital processing was applied to the raw optical signals that were acquired from the MAX30100 sensor. The following were some of the steps in the processing pipeline.

- **Step 1.** Reduce noise via a moving average filter with a window size of N (where $N = 10$) to reduce high-frequency noise while preserving temporal responsiveness using Equation (3). Additionally, to reduce sharp oscillations brought on by electrical or physiological noise, a digital low-pass filter was implemented.
- **Step 2.** Motion artifact suppression: To reduce the effect of finger or hand movement, signal stability was continuously monitored. The signals' standard deviation was calculated in a short time window; this level was defined to high deviations that invalidated the corresponding sample.
- **Step 3.** Ambient light compensation: The equipment was spectrophotometrically adjusted by recording the baseline readings in the absence of a finger to ensure that the signals that were recorded were solely those of blood and tissue absorption. These initial ambient values were retained as offsets to later measurements.

Digital filtering of the signal, motion artefact management, and ambient light management also enhanced the precision of the resulting glucose estimations and ensured reliable signal acquisition.

4.1. Custom algorithm and signal processing

A multi-stage signal-processing pipeline was used to achieve a proper noninvasive glucose estimation using the raw PPG signals obtained by the MAX30100 sensor. Each volunteer was recorded

for 30 seconds in both the red (660 nm) and the IR (880 nm) channels at 100 Hz. The subsequent bullet points summarize the custom algorithm applied in Arduino C++ on the microcontroller.

In the first stage of noise reduction and pre-processing, the crude optical data were initially filtered to eliminate high-frequency noise and electrical variations. The waveform was smoothed using a moving average filter ($N = 10$ samples) and then a first-order digital low-pass infinite impulse response (IIR) filter (0.8, cutoff frequency = 5 Hz). This dual-stage filtering process retained physiological pulsations but cancelled out sensor noise. The second stage of motion artifact suppression is available. To identify unstable or motion-corrupted blocks, the short-window standard deviation (M = 5 samples) was calculated on a continuous basis. The samples with more than 5% variation from the regional mean were automatically rejected, and the user was advised to reposition the finger. Ambient light interference was removed by subtracting a baseline level, which was obtained via pre-measurement readings without finger contact. In the third stage, AC/DC abstraction and feature computation, the infrared and red filtered signals were broken down into the AC component involving a pulsatile peak-to-peak amplitude in response to changes in the blood volume of the arteries, and the DC component involving nonpulsatile tissue and venous blood absorption, on the basis of Equation 2. The AC_RED signal was used to determine the HR from the peak detector and then averaged by a similar moving-average filter. The ratio R was then used to determine SpO_2 using the empirical relationship based on Equation (5) [64]. The values that were not within the normal physiological range (95–99) were automatically considered unreliable. In the final stage (the glucose estimation model), the estimate of glucose was finally given after a calibrated linear model was obtained from the 120-subject dataset. The value of the HR after filtering (HR_filt) was entered into Equation 4, where $a = 2.06$ and $b = -85.218$ are the regression coefficients between the two variables using the BM measurements as the dependent variable. Glucose estimation was only performed on valid samples that had a valid signal quality (normal SpO_2 and stable waveform). This was shown immediately on the LCD module. To achieve transparency and reproducibility, Table 1 outlines the major steps and parameters of the custom algorithm, which allows one to process the PPG at once.

$$SpO_2 = 110 - 25R \tag{5}$$

Table 1. Summary of each stage of the algorithm's steps, parameters, and effects.

Stage	Methods	Parameter	Effect
First	Moving average	$N = 10$ samples	Noise reduction and pre-processing
	First-order digital low-pass IIR filter	0.8, cutoff frequency = 5 Hz	Removing high-frequency noise
Second	Motion artifact	Standard deviation threshold = 5%	Flag unstable readings
	Ambient light interference	10 pre-measurements	Remove ambient light
Third	Abstraction	AC/DC abstraction in Equation 2	AC/DC abstraction and feature computation
Final	Glucose model	$a = 2.06$, $b = -85.218$ in Equation 4	Regression coefficients

5. Evaluation of proposed system based on statistical analyses

A commercial benchmark glucometer was used to test the recommended system (BM: Accu-Chek Active, Roche Diagnostics). Paired glucose values were also recorded using both methods from each subject at the same time, assuming the same conditions. Although the test values might have been represented in the readings of the proposed system, the actual reference values were the BM readings. Accuracy was computed as per the accepted validation procedures and was in accordance with Equations (6–9) [65,66]. Three statistical analyses were conducted to carry out a comprehensive analysis of performance. The standard deviation and mean absolute error were applied in the error test used to determine the mean difference between approaches. Bland–Altman analysis was used to determine the systematic bias and define the 95% limits of agreement. Clarke's error grid analysis was used to assess the clinical significance of difference in measurements, where Zones A and B in the range of values are deemed to be clinically acceptable [67,68]. Furthermore, diagnostic performance measures were also determined, namely sensitivity (SN), specificity (SP), accuracy, true positives (TP), true negatives (TN), false positives (FP), and false negatives (FN). Such measures can give analytical and clinical insights into the trustworthiness of the suggested system.

Every volunteer was quantified in just one instance and in identical conditions. The value only represents single glucose measurements of 120 volunteers as opposed to a time series of a single volunteer. In Figure 7, the *x*-axis indicates the index of samples and the *y*-axis indicates the concentration of glucose (mg/dL) after using both systems. In future work, continuous measurements (before and after a meal or an Oral Glucose Tolerance Test (OGTT) glucose tolerance test) will be taken into consideration. The BM reference device that was used in this study is illustrated in Figure 8. The joint statistical analyses proved that the proposed system exhibited a high rate of agreement with the BM device, with the deviations being within acceptable clinical ranges. Figure 9 shows the HR and SpO_2 values during measurements on the MAX30100 sensor in 120 volunteers of various ages. The HR values have a significant variation that is attributed to changing physiological values and blood glucose levels, and the SpO_2 values are mostly constant within the normal range of 95–99%. The fact that the PPG signals obtained by the sensor are sensitive to cardiovascular/metabolic variations proves that the suggested noninvasive measurement system is reliable. The *x*-axis shows the index of age in years, and the *y*-axis shows the measurements on the MAX30100.

To confirm the physiological assumptions of the proposed noninvasive glucose monitoring system, the data obtained from 120 subjects were subjected to a statistical analysis. The results of the Pearson correlation test showed that both HR and SpO_2 had a strong negative correlation ($r = -0.936$) that was highly significant ($p = 0.8 \times 10^{-55}$), which confirmed that a standard increase in cardiac workload is normally accompanied by a minor decrease in peripheral SpO_2. Moreover, there was a positive correlation between HR and blood glucose levels, and this correlation was strong. The linear regression model resulted in $R^2 = 0.860$, and the HR coefficient was very significant ($p = 2.74 \times 10^{-52}$). The model's parameters show that a 1 beat per minute (bpm) increase in the HR will result in an increase in glucose level of approximately 2.06mg/dL, with the intercept being −85.218 mg/dL. The findings confirm the linear model applied to the proposed system as physiologically plausible and statistically sound, where the SpO_2 is more of a signal quality control variable than a predictive variable. Even though SpO_2 was recorded along with HR, it was applied as a normalization and validation parameter in signal pre-processing, not as an input variable. It was also able to provide

stabilization in the PPG waveform and reduce motion and perfusion artifacts so that variations in the HR were a true indication of the real physiological changes related to glucose levels.

$$\text{Accuracy (\%)} = \frac{\text{True value} - \text{measured value}}{\text{True value}} \times 100\% \quad (6)$$

$$\text{Sensitivity (SN)} = \frac{TP}{TP+FN} \quad (7)$$

$$\text{Specificity (SP)} = \frac{TN}{TN+FP} \quad (8)$$

$$\text{Accuracy} = \frac{TP+TN}{TP+TN+FP+FN} \quad (9)$$

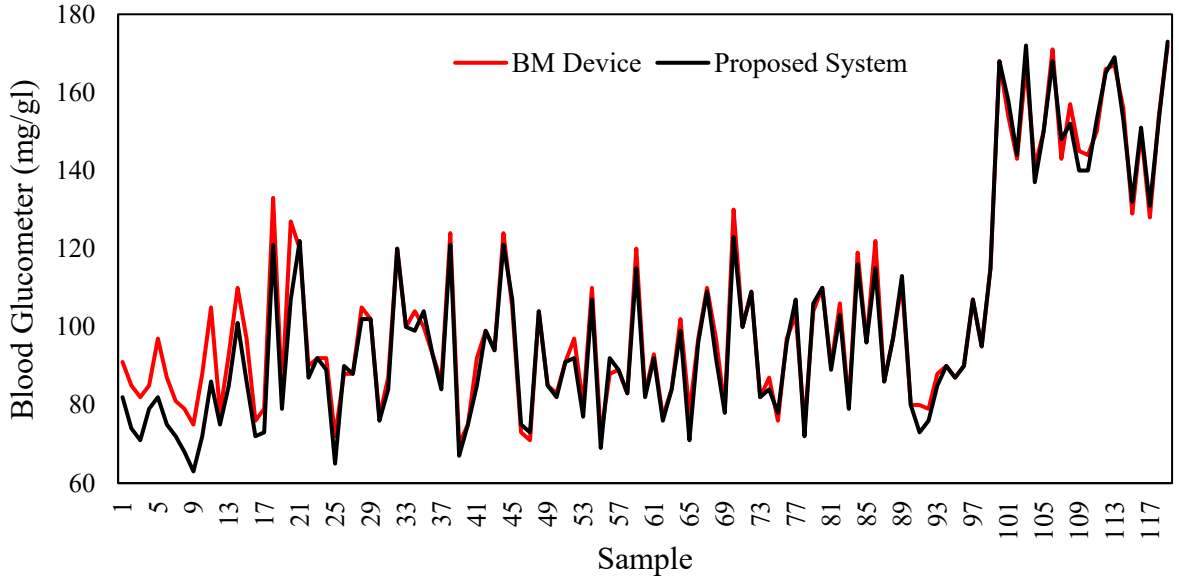

Figure 7. Blood glucose measurements (mg/dL) using the blood glucometer of the proposed system and the BM device.

Figure 8. The BM device.

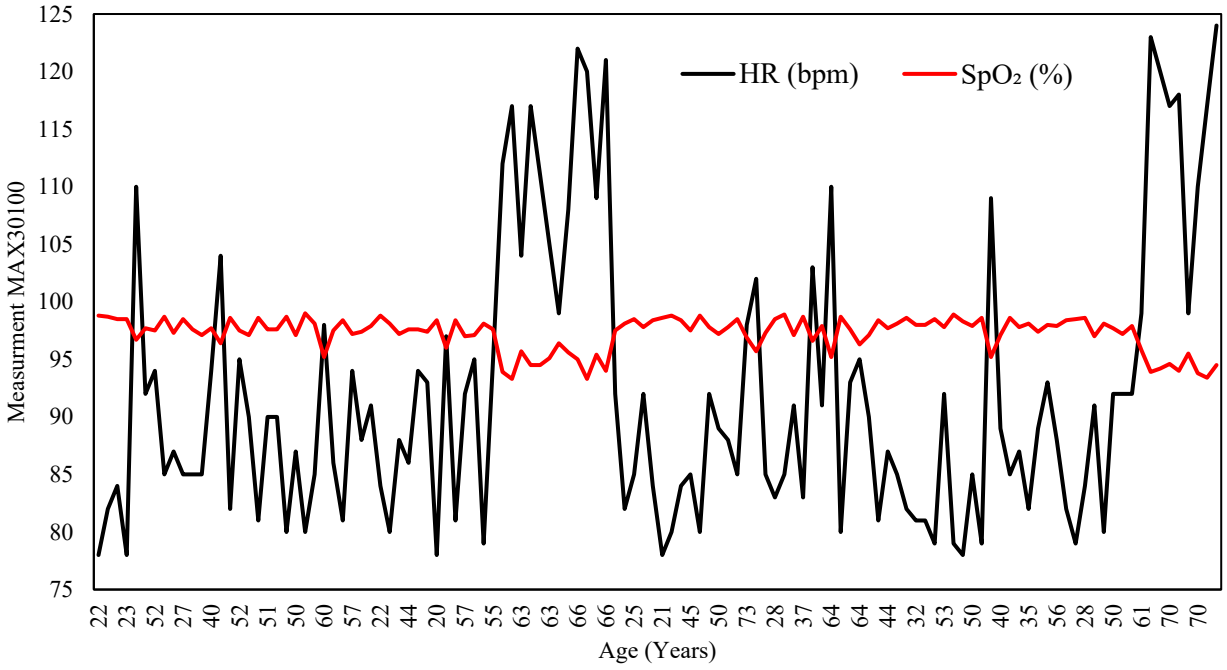

Figure 9. The variation in HR and SpO_2 with age.

5.1. Error test

The proposed system and the BM device were tested for convergence using the error test [69,70]. All 120 paired samples were used to calculate three error metrics: Mean absolute error (MAE), absolute percentage error (APE), and mean absolute percentage error (MAPE). The APE values varied from 0 to 19%, with a corresponding MAPE of 3.56%, according to the results, suggesting that the suggested system maintained a low relative error throughout the dataset. The absolute error also varied from 0 to 20 mg/dL, with an overall MAE of 3.65 mg/dL, which indicates a minor departure from the BM reference values. Figure 10a illustrates the relationship between the APE values and the number of samples, while Figure 10b presents the distribution of absolute error across all samples compared with the MAE. These results confirm that the proposed system achieves close agreement with the BM device, with error values remaining within clinically acceptable limits.

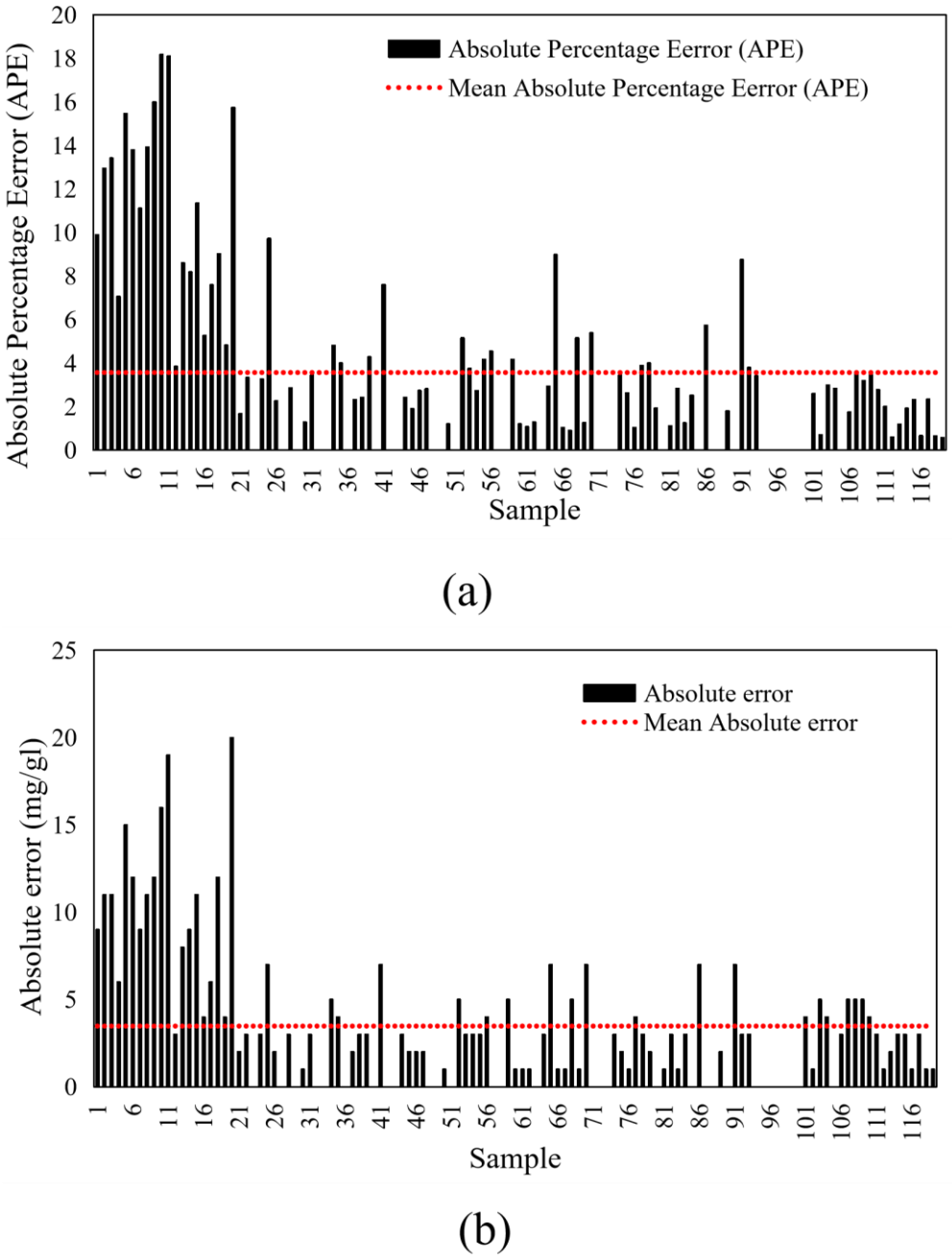

Figure 10. The relationship between the number of samples and (a) the APE and MAPE, and (b) the absolute error and MAE.

5.2. Bland–Altman test

Agreement between the proposed system and the BM device was further evaluated using Bland–Altman analysis [71,72]. Each paired measurement's error (mg/dL) was calculated as the discrepancy between the BM reference and the suggested system, 3.47 mg/dL was the mean error (μ), and 4.07 mg/dL was the standard deviation (σ). Using the definition of $\mu \pm 2\sigma$, the limits of agreement (LoA) were determined to be between −4.6 and 11.6 mg/dL. The fact that 97% of the data points fell inside

this range demonstrated a high degree of agreement between the two methods. A small percentage of the data points (black squares) are beyond the borders, but the majority (red circles) are inside the LoA, as seen in Figure 11. For noninvasive glucose monitoring, the overall LoA range of 16.2 mg/dL is within clinically acceptable tolerances. These results demonstrate that there is very little systematic bias, and that the suggested approach yields results that are closely aligned with the BM device.

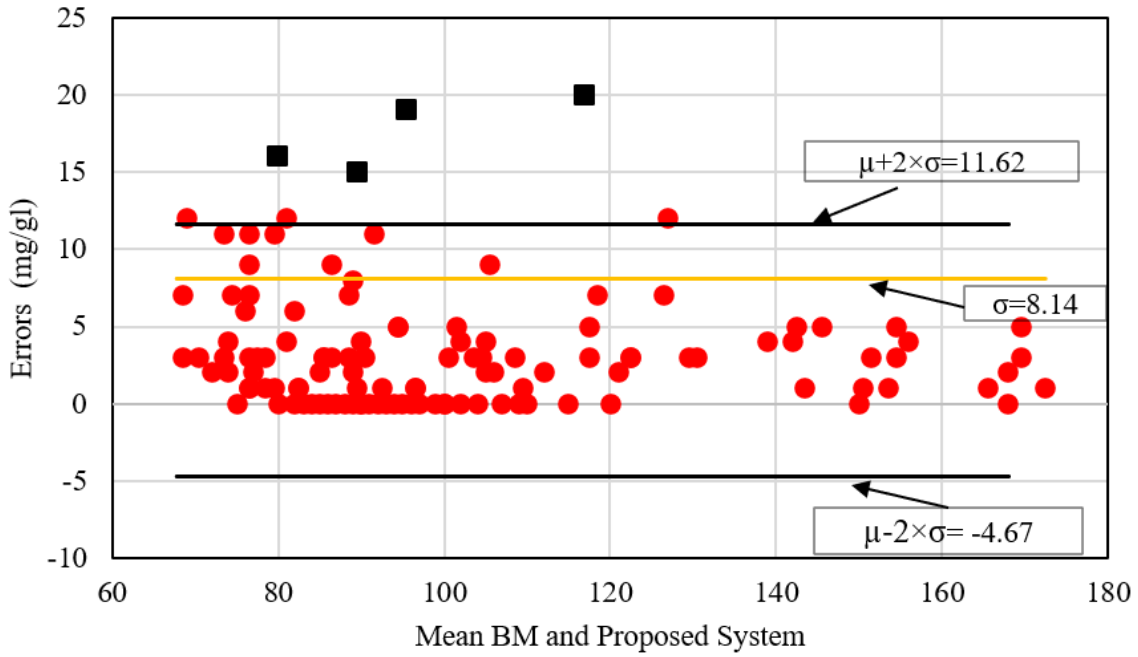

Figure 11. Bland–Altman plot for errors (mg/dL) between the mean from the BM and the proposed system.

5.3. Clarke error grid analysis

The Clarke error grid was used to evaluate the clinical accuracy of the proposed system by comparing its readings with those of the BM device [73,74]. In this analysis, the proposed system's values were plotted on the *x*-axis and the BM reference values on the *y*-axis (Figure 12). The grid is divided into five zones (A–E): Zone A, values within ±20% of the BM reference, and considered clinically accurate and acceptable; Zone B, values which fall outside a range of ±20% but not be sufficient to cause inappropriate clinical action; Zones C and D, values that have great error, since therapeutic decisions can be made incorrectly; Zone E, clinically dangerous and grossly inaccurate values.

The findings indicate high clinical reliability and consensus, whereby the majority of the paired measures (~96–98) fall in Zone A. All of them were in Zone B (only about 2–3%) and indicate some slight changes to be used in medicine. The percentage of data points in Zones C–E was below 1%, indicating that the system generates hardly any clinically inadvisable readings. Figure 11 has a blue diagonal line which depicts the line of absolute coincidence among the two devices, whereas the dashed green, orange, and red lines mark the boundaries of the zones. The fact that the red data points cluster around the diagonal in both Zones A and B indicates that the proposed system can give a measurement that is in line with the clinical accuracy requirement of noninvasive glucose monitoring.

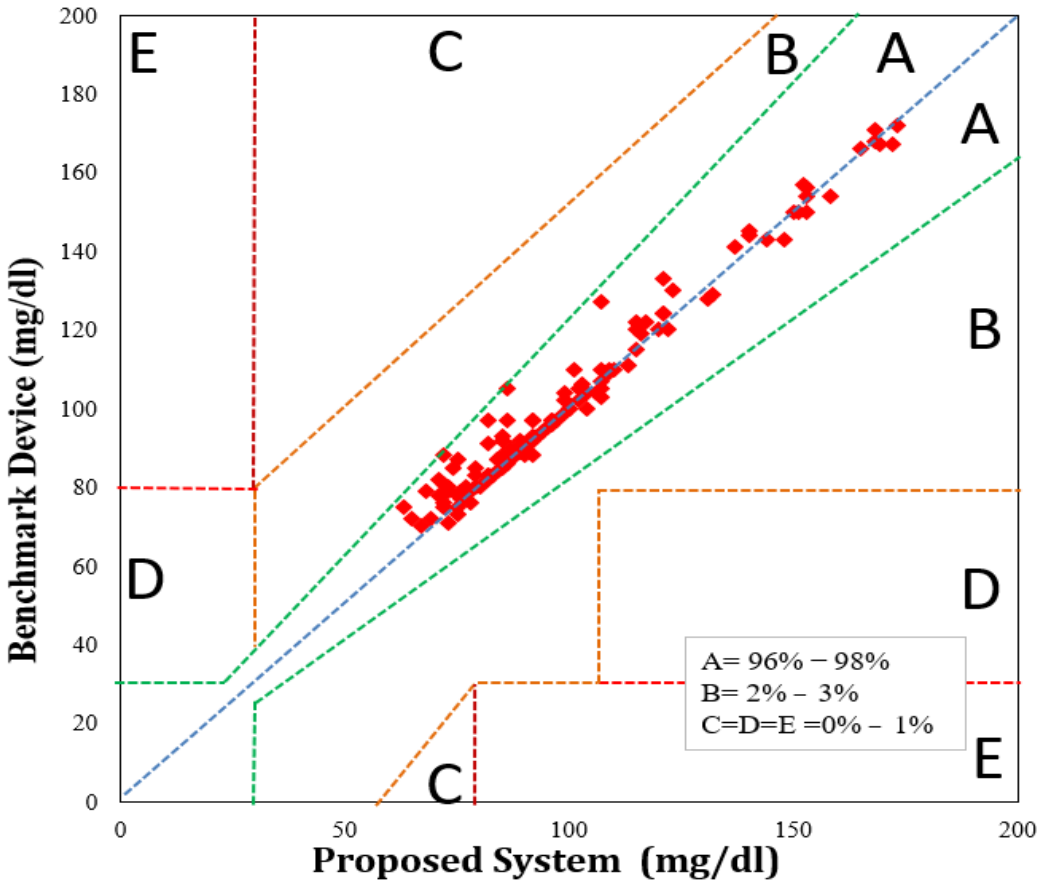

Figure 12. Clarke error grid analysis for the BM and the proposed system.

6. Results and discussion

The system was tested using 120 samples comprising 55 females and 65 males of different ages. The proposed device and a BM device (ACCU-CHEK) were used to test each participant simultaneously. The statistical testing revealed that the outputs of the proposed system were very similar to those of BM device. The key advantage of the suggested device is that it is noninvasive, so people will not experience the discomfort and inconvenience associated with finger-prick tests. The system offers quick and convenient blood glucose readings, and therefore can be used in daily monitoring at home and at work. This would hold significant clinical significance, since it would help the patients prevent abrupt changes in glucose that may result in such complications as hypertension and cardiac issues. Moreover, the device can assist in the minimization of long-term expenditure by lowering the number of laboratory check-ups and clinic visits (Figure 13). It is necessary to note that no protocols have been provided in this research for the handgrip test or any other physiological stress tests. The proposed system is based entirely on noninvasive optical measurements through a MAX30100 sensor placed on the fingertip.

The level of the system's performance was evaluated with the help of conventional measures of classification: TP, FP, TN, FN, SN, and SP. The values computed are TP = 95, TN = 22, FP = 1, and FN = 2. Using these values, the system had a sensitivity of 97.94, a specificity of 95.65, and an overall accuracy of 97.5. Moreover, statistical validation was done, using an error test, the Bland–Altman test,

and the Clarke error grid. The error test revealed small deviations between the proposed system and BM, with a MAE of 3.65 mg/dL and a MAPE of 3.56%. The Bland–Altman plot showed a high level of agreement with the BM equipment, with 97% of the samples lying within the agreement limits (−4.6 and 11.6 mg/dL) of both plots. The study with the Clarke error grid showed that <1% of the samples fell in Zones C and E and only 2–3% in Zone B, which demonstrates clinically credible results. On the other hand, 96–98% of samples were in Zone A. The results of the validation that confirmed the reliability of the system are summarized in Table 2 and demonstrated in Figure 14. The calibration investigation between the proposed system and the BM had an intercept of 5.6, a slope of 1.02, and a coefficient of determination (R^2) of 0.9714, which indicated there was a significant correlation. Finally, Table 3 compares the working of the proposed system with the past studies [22,23,27,28]. The proposed device recorded the best accuracy (~98%), which was higher than those reported by previous works that had an accuracy of 93%–96%. This shows the enhanced reliability and clinical capability of the developed system in relation to previous methods. The studies in [27,28] were closest to the proposed system in terms of the use of components, but they lacked the number of samples, achieving lower accuracy than the proposed system (94.3% and 93.97%, respectively). Table 3 provides a comparison between the proposed system and the previous studies according to the number of wavelengths that are used in them (the proposed system used two wavelengths (880 and 660 nm)). As it is possible to observe, the proposed system was more accurate than the previous ones. The better signal processing algorithm and the calibration of the device with a BM explain this.

One limitation of this study is that it did not address the analysis of HRV indicators. Although HRV analysis has proven its clinical significance in many studies, the proposed system was based solely on HR and SpO_2 for glucose estimation. In the future, HRV indicators could be integrated into the system to expand the scope of analysis and increase the reliability of the results.

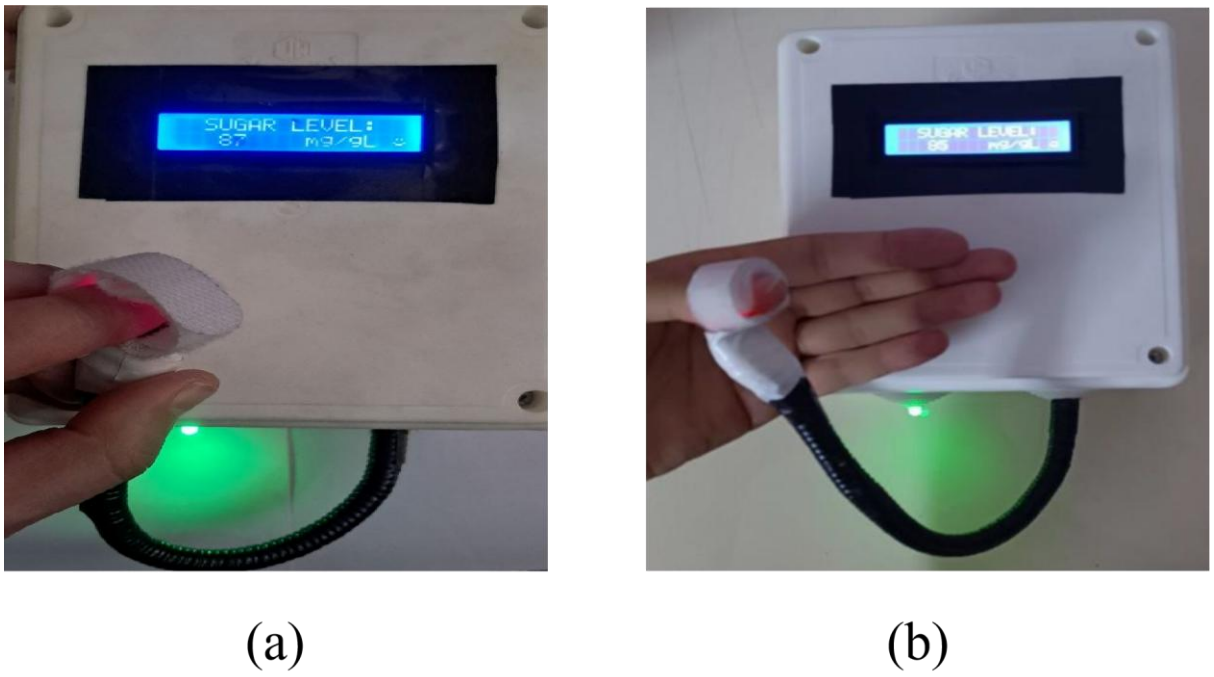

Figure 13. Snapshot of a result with the proposed system.

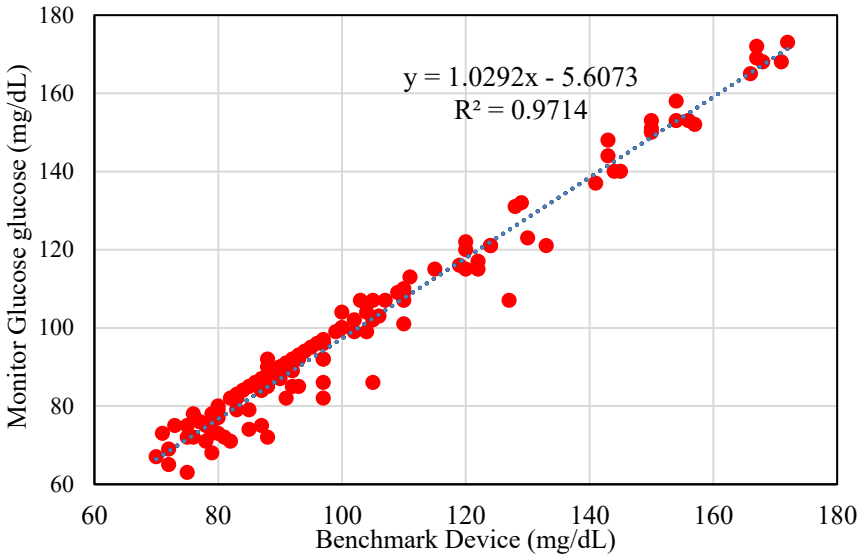

Figure 14. Calibration between the BM and the proposed system.

Table **2**. Summary of the statistical validation results for the proposed system compared with the BM device.

Method	Metric	Result	Interpretation
Error test	Mean absolute error (MAE)	3.65 mg/dL	Low average deviation from the BM
	Mean absolute percentage error (MAPE)	3.56%	High consistency across samples
	Absolute percentage error (APE) range	0 – 19%	Within acceptable limits
Bland–Altman analysis	Mean error (μ)	3.47 mg/dL	Small systematic bias
	Standard deviation (σ)	4.07 mg/dL	Low dispersion
	Limits of agreement (μ ± 2σ)	–4.6 to 11.6 mg/dL (97% of data)	Strong agreement with the BM
Clarke error grid	Zone A	~96–98%	Clinically accurate
	Zone B	~2–3%	Minor deviations, acceptable
	Zones C–E	<1%	Rare unsafe readings
Classification metrics	True positive (TP)	95	Correctly detected elevated glucose
	True negative (TN)	22	Correctly detected normal glucose
	False positive (FP)	1	Minimal misclassification risk
	False negative (FN)	2	Very low rate of missed cases
	Sensitivity (SN)	97.94%	High ability to detect positives
	Specificity (SP)	95.65%	High ability to detect negatives
	Accuracy	97.50%	Overall high classification accuracy

Table **3**. Comparison of previous studies and the current research.

Reference and year	Accuracy (%)	Method	Advantages	Disadvantages
[22] 2020	95	TCRT1000 optical sensor	Low cost, simple design, real-time results	Single wavelength and no algorithm
[23] 2024	96	Laser	IoT remote monitoring.	Needs to be calibrated frequently, does not model physiologically
[25] 2023	94–96	Microwave resonator	Low cost	Affected by ambient light
[26] 2021	95	Microwave resonator	Low cost	Affected by ambient light
[27] 2025	94.3	MAX30100	Inexpensive educational prototype, and easy to implement and simple design	Poor repeatability and validity of the data
[28] 2024	93.97	MAX30102	Wireless data transmission through an IoT module, portable and low power	
Proposed system	97.5	MAX30100	Dual wavelength sensing, physiological correlation, noise-insensitive	Moderate, did not analyze HRV

7. Conclusions

Diabetes is one of the most common diseases that continue to plague the world and, when uncontrolled, may largely affect the overall health of the individual. This study presented an alternative method of measuring blood glucose levels with a noninvasive device using an optical sensor (MAX30100), which is Arduino-based and does not require finger-prick techniques. The system was tested on 120 volunteers and compared with a reference device (BM). The high accuracy of the system (98%) was verified by statistical studies, such as error analysis, the Bland–Altman test, and the Clarke error grid, with majority of the studies falling within the clinically acceptable zone. The experiment

confirmed that the MAX30100 optical biosensor could be used in monitoring glucose-related physiological changes. The system has unique benefits that include pain-free operation, ease of use, quick measurement, and suitability for everyday self-monitoring. Its validity is better than other similar studies, which proves that it is a valid tool for diabetes management. Further developments are underway in terms of large-scale clinical validation, connection to mobile health interfaces and wearable systems, and cloud-based data management. Other capabilities like automated dietary reminders, reporting data to medical professionals, and a mobile application to check and communicate with the doctor will also be introduced.

Acknowledgments

The authors would like to thank the Electrical Engineering Technical College at Middle Technical University in Baghdad, Iraq, for assisting them in carrying out the experiments.

Ethical approval

No invasive procedures or biological samples were involved in this study, and it did not involve any medical procedures or the use of identifiable personal information. The sensor commercially available in the form of MAX30100 was used to record only noninvasive optical measurements (PPG signals: HR and SpO_2). No photos, fingerprints, faces, or biometric data of the volunteers were documented at any point, and all the data were completely anonymized before analysis. The study did not require formal approval by an institutional review board or ethical committee according to the institutional guidelines and ethics as stipulated in the Declaration of Helsinki on minimal-risk human research. Complete information regarding the objective and methods of the study was provided and verbal informed consent was given before participating. It was a voluntary activity, and the volunteers were not bound to attend in any way.

Conflict of interest

The authors declare no conflict of interest related to this study.

References

1. Holt RIG and Flyvbjerg A (2024) *Textbook of Diabetes,* USA: John Wiley & Sons.
2. Zakir F, Mohapatra S, Farooq U, et al. (2022) Introduction to metabolic disorders, In: Dureja H, Narasimha Murthy S, Wich PR, et al. *Drug Delivery Systems for Metabolic Disorders,* USA: Academic Press, 1–20. https://doi.org/10.1016/B978-0-323-99616-7.00001-3
3. Del Prato S, Bianchi C, Daniele G (2024) Abnormalities of insulin secretion and β-cell defects in type 2 diabetes, In: Holt RIG and Flyvbjerg A, *Textbook of Diabetes,* USA: John Wiley & Sons, 225–237. https://doi.org/10.1002/9781119697473.ch16
4. Kitabchi AE, Umpierrez GE, Miles JM, et al. (2009) Hyperglycemic crises in adult patients with diabetes. *Diabetes Care* 32: 1335. https://doi.org/10.2337/dc09-9032
5. Umpierrez GE, Davis GM, ElSayed NA, et al. (2024) Hyperglycemic crises in adults with diabetes: a consensus report. *Diabetes care* 47: 1257–1275. https://doi.org/10.2337/dci24-0032

6. Susan van D, Beulens JWJ, Yvonne T. van der S, et al. (2010) The global burden of diabetes and its complications: an emerging pandemic. *Eur J Cardiov Prev R* 17: s3–s8. https://doi.org/10.1097/01.hjr.0000368191.86614.5a
7. Cousin E, Duncan BB, Stein C, et al. (2022) Diabetes mortality and trends before 25 years of age: an analysis of the global burden of disease study 2019. *Lancet Diabetes Endocrinol* 10: 177–192. https://doi.org/10.1016/S2213-8587(21)00349-1
8. Moses JC, Adibi S, Wickramasinghe N, et al. (2024) Non-invasive blood glucose monitoring technology in diabetes management. *Mhealth* 10: 9. https://doi.org/10.21037/mhealth-23-9
9. Jenkins K (2014) II. Needle phobia: a psychological perspective. *Brit J Anaesth* 113: 4–6. https://doi.org/10.1093/bja/aeu013
10. Holt RI, Cockram CS, Ma RC, et al. (2024) Diabetes and infection: review of the epidemiology, mechanisms and principles of treatment. *Diabetologia* 67: 1168–1180. https://doi.org/10.1007/s00125-024-06102-x
11. Cebedio MC, Rabioglio LA, Gelosi IE, et al. (2020) Analysis and design of a microwave coplanar sensor for non-invasive blood glucose measurements. *IEEE Sens J* 20: 10572–10581. https://doi.org/10.1109/JSEN.2020.2993182
12. Ebrahimi A, Scott J, Ghorbani K (2020) Microwave reflective biosensor for glucose level detection in aqueous solutions. *Sens Actuators A* 301: 111662. https://doi.org/10.1016/j.sna.2019.111662
13. Buford RJ, Green EC, McClung MJ (2021) A microwave frequency sensor for non-invasive blood-glucose measurement, *2008 IEEE sensors applications symposium,* IEEE, 2008: 4–7. https://doi.org/10.1109/SAS.2008.4472932
14. Meaney PM, Gregory AP, Seppälä J, et al. (2016) Open-ended coaxial dielectric probe effective penetration depth determination. *IEEE T Microw Theory* 64: 915–923. https://doi.org/10.1109/TMTT.2016.2519027
15. Juan CG, Bronchalo E, Potelon B, et al. (2019) Glucose concentration measurement in human blood plasma solutions with microwave sensors. *Sensors* 19: 3779. https://doi.org/10.3390/s19173779
16. Mohammadi P, Mohammadi A, Demir S, et al. (2021) Compact size, and highly sensitive, microwave sensor for non-invasive measurement of blood glucose level. *IEEE Sens J* 21: 16033–16042. https://doi.org/10.1109/JSEN.2021.3075576
17. Venkataraman J and Freer B (2011) Feasibility of non-invasive blood glucose monitoring: In-vitro measurements and phantom models, *2011 IEEE international symposium on antennas and propagation (APSURSI),* IEEE, 2011: 603–606. https://doi.org/10.1109/APS.2011.5996782
18. Kiani S, Rezaei P, Fakhr M (2024) Investigation of microwave resonant sensors for use in detecting changes of noninvasive blood glucose concentration. *Org Inorg Mater Based Sens* 3: 1055–1064. https://doi.org/10.1002/9783527834266.ch45
19. Park C, Park DY, Zhang H, et al. (2025) Adaptive electronics for photovoltaic, photoluminescent and photometric methods in power harvesting for wireless wearable sensors. *Nat Commun* 16: 5808. https://doi.org/10.1038/s41467-025-60911-1
20. Hanna J, Bteich M, Tawk Y, et al. Noninvasive, wearable, and tunable electromagnetic multisensing system for continuous glucose monitoring, mimicking vasculature anatomy. *Sci Adv* 6: eaba5320. https://doi.org/10.1126/sciadv.aba5320

21. Yilmaz T, Foster R, Hao Y (2019) Radio-frequency and microwave techniques for non-invasive measurement of blood glucose levels. *Diagnostics* 9: 6. https://doi.org/10.3390/diagnostics9010006
22. Anupongongarch P, Kaewgun T, O'Reilly JA (2020) Design and construction of a non-invasive blood glucose meter. Available from: https://www.ijabme.net/journal/ijabme_13_2_4.pdf.
23. Alam I, Dunde A, Balapala KR, et al. (2024) Design and development of a non-invasive opto-electronic sensor for blood glucose monitoring using a visible light source. *Cureus* 16: e60745. https://doi.org/10.7759/cureus.60745
24. Shi J, Fernández-García R, Gil I (2025) Sensor technologies for non-invasive blood glucose monitoring. *Sensors* 25: 3591. https://doi.org/10.3390/s25123591
25. Kiani S and Rezaei P (2023) Microwave substrate integrated waveguide resonator sensor for non-invasive monitoring of blood glucose concentration: low cost and painless tool for diabetics. *Measurement* 219: 113232. https://doi.org/10.1016/j.measurement.2023.113232
26. Kiani S, Rezaei P, Fakhr M (2021) Dual-frequency microwave resonant sensor to detect noninvasive glucose-level changes through the fingertip. *IEEE T Instrum Meas* 70: 1–8. https://doi.org/10.1109/TIM.2021.3052011
27. Herlambang B and Arifin F (2025) Design of a non-invasive blood sugar level measuring instrument using arduino nano and MAX30100 sensor module. *Res Intell Manuf Assem* 4: 283–290. https://doi.org/10.25082/RIMA.2025.02.005
28. Islamudin AF, Rahmawati T, Triwiyanto T, et al. (2024) Improvement of non-invasive blood sugar and cholesterol meter with IoT technology. *Jurnal Teknokes* 17: 63–68. https://doi.org/10.35882/teknokes.v17i1.666
29. Du K, Li J, Huang Z, et al. (2024) A non-invasive blood glucose detection system based on photoplethysmogram with multiple near-infrared sensors. *IEEE J Biomed Health* 29: 2496–2505. https://doi: 10.1109/JBHI.2024.3443317
30. Ali S, Shakeel A, Khan FH, et al. (2024) Development and evaluation of a sensor-based non-invasive blood glucose monitoring system using near-infrared spectroscopy. *Eng Proc* 82: 19. https://doi.org/10.3390/ecsa-11-20395
31. Suprayitno EA, Setiawan A, Dijaya R (2018) Design of instrumentation in detecting blood sugar levels with non-invasive technique base on IoT (Internet of Things). *Int J Eng Technol* 7: 440–442. https://doi.org/10.14419/ijet.v7i4.15.25252
32. Pires LM and Martins J (2024) Design and implementation of a low-power device for non-invasive blood glucose. *Designs* 8: 63. https://doi.org/10.3390/designs8040063
33. Xu X, Jin X, Xiao D, et al. (2023) A hybrid autoregressive fractionally integrated moving average and nonlinear autoregressive neural network model for short-term traffic flow prediction. *J Intell Transp Syst* 27: 1–18. https://doi.org/10.1080/15472450.2021.1977639
34. Soleymaani F, Sandidzadeh MA, Mirabadi A (2024) Calibrating the train position and speed in signalling systems using balises and wireless sensor networks. *Int J Sens Ne* 46: 100–113. https://doi.org/10.1504/IJSNET.2024.141785
35. Vettori S, Di Lorenzo E, Peeters B, et al. (2023) An adaptive-noise augmented kalman filter approach for input-state estimation in structural dynamics. *Mech Syst Signal Process* 184: 109654. https://doi.org/10.1016/j.ymssp.2022.109654

36. Rahim NA and Othman N (2024) Development of IoT-based heatstroke early symptoms monitoring system for students in malaysia. *Evol Electr Electron Eng* 5: 91–101. https://doi.org/10.30880/eeee.2024.05.01.012
37. Ranjith R, Priya S, Kaviya Dharshini AS, et al. (2024) Non-invasive hemoglobin measurement using optical method. *Heliyon* 10: e35777. https://doi.org/10.1016/j.heliyon.2024.e35777
38. Pintavirooj C, Ni B, Chatkobkool C, et al. (2021) Noninvasive portable hemoglobin concentration monitoring system using optical sensor for anemia disease. *Healthcare* 9: 647. https://doi.org/10.3390/healthcare9060647
39. Quaresima V, Ferrari M, Scholkmann F (2024) Ninety years of pulse oximetry: history, current status, and outlook. *J Biomed Opt* 29: S33307–S33307. https://doi.org/10.1117/1.JBO.29.S3.S33307
40. Fakhri AB, Jameel HF, Mahmood MF (2022) Management patients information based finger print. *Indones J Electr Eng Comput Sci* 26: 1281–1289. https://doi.org/10.11591/ijeecs.v26.i3.pp1281-1289
41. Adami C (2024) Monitoring oxygenation, In: Lamont L, Grimm K, Robertson S, et al. *Veterinary Anesthesia and Analgesia: The Sixth Edition of Lumb and Jones*, USA: John Wiley & Sons, 231–239. https://doi.org/10.1002/9781119830306.ch15
42. Saucier MA (2024) Near infrared and shortwave infrared dyes for biological imaging, bloodstain detection, and optoelectronic applications [PhD thesis]. USA: The University of Mississippi.
43. Deepika K, Vedanth K, Tejesh K (2024) Blood Oxygen and heart rate monitor with Max30100 and arduino. Available from: https://materialsciencetech.com/mst/uploads/2024-42649.pdf.
44. Peng Z and Yang Z (2024) Optical blood glucose non-invasive detection and its research progress. *Analyst* 149(19): 4830–4841. https://doi.org/10.1039/D4AN01048E
45. Jarnda KV, Dai H, Ali A, et al. (2025) A review on optical biosensors for monitoring of uric acid and blood glucose using portable POCT devices: status, challenges, and future horizons. *Biosensors* 15: 222. https://doi.org/10.3390/bios15040222
46. Wang X, Li Z, Su L (2024) Soft optical waveguides for biomedical applications, wearable devices, and soft robotics: a review. *Adv Intell Syst* 6: 2300482. https://doi.org/10.1002/aisy.202300482
47. Almoutairi MO, Almatrafi NF, Faydah NS, et al. (2024) Noninvasive blood glucose monitoring with optical coherence tomography. *J Int Crisis Risk Commun Res* 7: 3156–3160. https://doi.org/10.63278/jicrcr.vi.2637
48. Korbee N, Figueroa FL, Aguilera J (2005) Effect of light quality on the accumulation of photosynthetic pigments, proteins and mycosporine-like amino acids in the red alga Porphyra leucosticta (Bangiales, Rhodophyta). *J Photochem Photobiol B* 80: 71–78. https://doi.org/10.1016/j.jphotobiol.2005.03.002
49. Borse V, Konwar AN, Buragohain P (2020) Oral cancer diagnosis and perspectives in India. *Sens Int* 1: 100046. https://doi.org/10.1016/j.sintl.2020.100046
50. Ibe PC (2023) A comparative study for real time and remote heart-rate measurement using max30100 and pulse sensor based devices. Available from: https://acikerisim.gelisim.edu.tr/server/api/core/bitstreams/14a50fc4-568e-4121-aa03-d8b4c8dd26a6/content.
51. Wu X, Huang D, Lin Q, et al. (2025) Thermally stable broadband Cr^{3+}-doped $RbAl_3P_6O_{20}$ phosphor for near-infrared spectroscopy applications. *Inorg Chem* 64: 3476–3484. https://doi.org/10.1021/acs.inorgchem.4c05081

52. Yin Y, Dai J, Wang B, et al. (2025) Wearable noninvasive glucose biosensors: biological metabolism, chemical sensing, and biological applications. *Adv Mater Technol* 2025: e01311. https://doi.org/10.1002/admt.202501311
53. Lin JJ, Huang DY, Hong ML, et al. (2024) An ultra-wideband metamaterial absorber ranging from near-infrared to mid-infrared. *Photonics* 11: 939. https://doi.org/10.3390/photonics11100939
54. Keithellakpam LB, Danielski R, Singh CB, et al. (2025) A comprehensive review on minimally destructive quality and safety assessment of agri-food products: chemometrics-coupled mid-infrared spectroscopy. *Foods* 14: 3805. https://doi.org/10.3390/foods14223805
55. Acton JM (2025) The survivability of nuclear command-and-control capabilities. *J Strategic Stud* 48: 407–464. https://doi.org/10.1080/01402390.2024.2435957
56. Zakaria AA, Allam A, AbdelRahman AB (2025) Microwave based non-invasive blood glucose sensors: key design parameters and case-informed evaluation. *IEEE Access* 13: 154695–154711. https://doi.org/10.1109/ACCESS.2025.3598618
57. Mishra PK, Singh T, Tripathi VS (2024) A rectangular dielectric resonator based microwave sensor for non-invasive blood glucose sensing applications. *Sens Imaging* 25: 35. https://doi.org/10.1007/s11220-024-00486-1
58. Arabboev M, Begmatov S, Rikhsivoev M, et al. (2024) A review on blood glucose monitoring systems and devices. *Eurasian J Math Theory Comput Sci* 4: 7–13. https://doi.org/10.21014/actaimeko.v13i1.1679
59. Jananee MG (2023) SpO_2 and temperature measurement device based on ATmega328p microcontroller chip with mobile connection for real-time monitoring. Available from: https://acikerisim.gelisim.edu.tr/server/api/core/bitstreams/2e775581-2ca3-4339-bc7e-ae6aaa37ed41/content.
60. Mahmood MF, Jameel HF, Hammed MAN (2022) Measurement of an electroretinogram signal and display waves on graphical user interface by laboratory virtual instrument engineering workbench. *Indones J Electr Eng Comput Sci* 25: 980–988. https://doi.org/10.11591/ijeecs.v25.i2.pp980-988
61. Mahmood MF, Mohammed SL, Gharghan SK, et al. (2020) Design and implementation of wireless power transfer for wireless heart rate monitoring system, *2020 13th International Conference on Developments in eSystems Engineering (DeSE)*, IEEE, 2020: 453–458. https://doi.org/10.1109/DeSE51703.2020.9450792
62. Hashim H, Mohammed S, Gharghan S (2019) Accurate localization of elderly people based on neural and wireless sensor networks. *J Eng Appl Sci* 14: 3777–3789. https://doi.org/10.36478/jeasci.2019.3777.3789
63. Jameel HF, Mahmood MF, Yaseen SM (2022) Design and implementation of a peristaltic pump based on an air bubble sensor. *Int J Bioautom* 26: 361. https://doi.org/10.7546/ijba.2022.26.4.000866
64. Lyimo RS and Ngulugulu A (2025) A portable and affordable Photoplethysmography (PPG)-based health monitoring solution for low-resource settings. *J Res Innov Implic Educ* 9: 964–973. https://doi.org/10.59765/vhry46r
65. Reza S, Haldar A, Khan SK, et al. (2024) Validation of water quality parameters using ion balancing and electrochemical approaches: a case study. *Int J Environ Anal Chem* 2024: 1–20. https://doi.org/10.1080/03067319.2024.2426739

66. Huang AA and Huang SY (2024) Comparison of model feature importance statistics to identify covariates that contribute most to model accuracy in prediction of insomnia. *Plos One* 19: e0306359. https://doi.org/10.1371/journal.pone.0306359
67. Mahmood MF (2024) Recognition and categorization of blood groups by machine learning and image processing method. *Innovative Biosyst Bioeng* 8: 53–68. https://doi.org/10.20535/ibb.2024.8.2.298201
68. Wahba MA, Ashour AS, Ghannam R (2020) Prediction of harvestable energy for self-powered wearable healthcare devices: filling a gap. *IEEE Access* 8: 170336–170354. https://doi.org/10.1109/ACCESS.2020.3024167
69. Ahmed AH, Ahmad S, Abu Sayed M, et al. (2023) Predicting the possibility of student admission into graduate admission by regression model: a statistical analysis. *J Math Stat Stud* 4: 97–105. https://doi: 10.32996/jmss.2023.4.4.10
70. Mamenko M, Lysikova DV, Spires DR, et al. (2022) Practical notes on popular statistical tests in renal physiology. *Am J Physiol-Renal* 323: F389–F400. https://doi.org/10.1152/ajprenal.00427.2021
71. Li Y, He X, Li D, et al. (2025) Bland-Altman plot to assess the consistency of arterial and venous blood lactate in the emergency room: a retrospective cohort study. *Sci Rep* 15: 2143. https://doi.org/10.1038/s41598-025-85104-0
72. Mahmood MF, Mohammed SL, Gharghan SK, et al. (2020) Wireless power transfer based on spiral ‐ spider coils for a wireless heart rate sensor, *2020 13th International Conference on Developments in eSystems Engineering (DeSE)*, IEEE, 2020: 183–188.
73. Klonoff DC, Freckmann G, Pleus S, et al. (2024) The diabetes technology society error grid and trend accuracy matrix for glucose monitors. *J Diabetes Sci Technol* 18: 1346–1361. https://doi.org/10.1177/19322968241275701
74. Jokari R, Mahyari Z, Moulodi MJ, et al. (2025) An infrared non-invasive system for measuring blood glucose: a primary study using serum samples. *J Biomed Phys Eng* 15: 385–392. https://doi.org/10.31661/jbpe.v0i0.2305-1618

AIMS Press